The Astrophysical Journal, 848:86 (13pp), 2017 October 20 https://doi.org/10.3847/1538-4357/aa8a71

A Tale of Two Impostors: SN2002kg and SN1954J in NGC 2403*

Roberta M. Humphreys[1], Kris Davidson[1], Schuyler D. Van Dyk[2], and Michael S. Gordon[1]
[1] Minnesota Institute for Astrophysics, 116 Church St. SE, University of Minnesota, Minneapolis, MN 55455, USA; roberta@umn.edu
[2] Caltech/IPAC, Mailcode 100-22, Pasadena, CA 91125, USA
Received 2017 July 28; revised 2017 September 1; accepted 2017 September 1; published 2017 October 17

Abstract

We describe new results on two supernova impostors in NGC 2403, SN 1954J(V12) and SN 2002kg(V37). For the famous object SN 1954J, we combine four critical observations: its current SED, its Hα emission line profile, the Ca II triplet in absorption in its red spectrum, and the brightness compared to its pre-event state. Together, these strongly suggest that the survivor is now a hot supergiant with $T \sim 20{,}000$ K, a dense wind, substantial circumstellar extinction, and a G-type supergiant companion. The hot star progenitor of V12's giant eruption was likely in the post-red supergiant stage and had already shed a lot of mass. V37 is a classical LBV/S Dor variable. Our photometry and spectra observed during and after its eruption show that its outburst was an apparent transit on the HR Diagram due to enhanced mass loss and the formation of a cooler, dense wind. V37 is an evolved hot supergiant at $\approx 10^6\ L_\odot$ with a probable initial mass of 60–80 $M_\odot$.

Key words: stars: massive – stars: variables: S Doradus – supernovae: individual (SN1954J, SN2002kg)

1. Introduction

Massive star "eruptions" basically fall into two categories: normal Luminous Blue Variable (LBV)/S Doradus variability and giant eruptions with super-Eddington luminosities and massive radiation-driven outflows (Humphreys & Davidson 1994; Davidson 2016; Owocki & Shaviv 2016). In a giant eruption, the total luminosity substantially increases. The energetics of the giant eruptions, the duration, and what we observe are quite different from LBV/S Dor variability. The so-called LBV eruption is due to an increased mass-loss rate, which causes the wind to become dense and opaque with a large, cooler pseudo-photosphere and no substantial increase in luminosity in most cases. This enhanced mass-loss state can last for several years. The origin of the instability, their progenitors, and evolutionary state of the giant eruptins and the classical LBVs may also be different.

The numerous transient surveys are finding an increasing number of what appear to be nonterminal giant eruptions, apparently from evolved very massive stars. Many of these giant eruptions are spectroscopically similar to the Type IIn supernovae and thus receive an SN designation, but are later recognized as subluminous or their spectra and light curves do not develop like true supernovae. Consequently, they are often referred to as "supernova impostors" (see Van Dyk & Matheson 2012b for a review). This is a diverse group of objects with a range of luminosities and possible progenitors. A few impostors appear to be normal LBV/S Dor variables in the eruptive or maximum light state, while most are giant eruptions possibly similar to η Car (Humphreys & Davidson 1994). Of course the true test of an impostor is that it survives the giant eruption. Three of the four historical examples, η Car, P Cyg, and SN1954J (Humphreys. et al. 1999; Van Dyk et al. 2005b), survived their giant eruptions while the fourth, SN1961V, is still controversial (Kochanek et al. 2011; Van Dyk & Matheson 2012a).

Here we present recent spectra and photometry for two supernova impostors in the nearby spiral NGC 2403: SN1954J (V12) and SN2002kg(V37). Both received supernova designations, but instead are examples of nonterminal, high mass-loss episodes. SN2002kg's eruption was subluminous and it was quickly recognized as a nonsupernova. It was identified with the "irregular blue variable" V37 in NGC 2403 (Tammann & Sandage 1968), an LBV/S Dor variable in its maximum light stage (Van Dyk 2005a; Weis & Bomans 2005). Van Dyk et al. (2006) and Maund et al. (2006) have discussed its spectra and photometry during its 2002–2004 maximum.

SN1954J is famous. Based on its peculiar light curve (Tammann & Sandage 1968) and its resemblance to η Car and SN1961V, it was also considered another possible example of Zwicky's Type V supernovae (Kowal et al. 1972), but it is also known as V12 in NGC 2403 (Tammann & Sandage 1968). Like V37, it was also described as an irregular blue variable. Humphreys & Davidson (1994) and Humphreys. et al. (1999) included it as one of four examples of a giant eruption or η Car-like variable. *HST* imaging (Van Dyk et al. 2005b) resolved V12 into four stars, one of which is very bright in Hα.[3] Van Dyk et al. (2005b) also obtained an echellette spectrum with the Keck-II telescope, albeit with low S/N, that showed an Hα emission profile with broad wings similar to that of η Car. They thus argued convincingly that this Hα bright object, star 4, is most likely the survivor.

Our new observations are described in the next section. In Section 3, we discuss V37's eruption and post-eruption spectra, its luminosity, and its light curve. The analysis of V12's current spectrum and photometry and its light curve is less straightforward. In addition to the Hα emission with a Thomson scattering profile, the red spectrum shows strong Ca II absorption lines

* Based on observations with the Multiple Mirror Telescope, a joint facility of the Smithsonian Institution and the University of Arizona, and on observations obtained with the Large Binocular Telescope (LBT), an international collaboration among institutions in the United States, Italy, and Germany. LBT Corporation partners include The University of Arizona on behalf of the Arizona university system; Istituto Nazionale di Astrofisica, Italy; LBT Beteiligungsgesellschaft, Germany, representing the Max-Planck Society, the Astrophysical Institute Potsdam, and Heidelberg University; The Ohio State University, and The Research Corporation, on behalf of The University of Notre Dame, University of Minnesota, and University of Virginia.

[3] See Figure 8 in Van Dyk et al. (2005b). The Hα image is reproduced here in Figure 1.

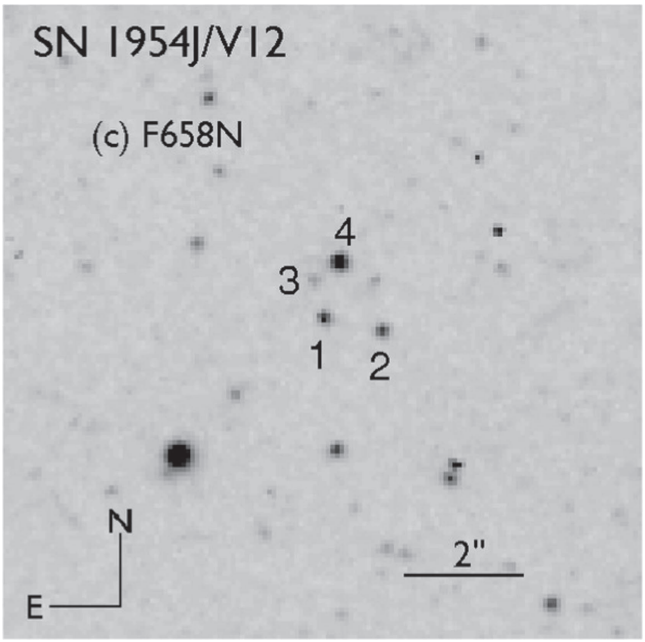

Figure 1. Environment of V12/SN 1954j. The Hα *HST* image from Van Dyk et al. (2005b) showing the four stars.

typical of a G-type supergiant. V12's most puzzling characteristic is the decline in the luminosity of the apparent survivor compared with the pre-eruption object. We describe V12's pre- and post-eruption characteristics, the evidence for circumstellar dust and the probable nature of the progenitor in Section 4. In the final section, we summarize our conclusions for the progenitors and surviving stars in each case.

2. The Observations

2.1. Spectroscopy

Post-eruption spectra of V37 were observed on 2012 October 10 and on 2012 December 4 and 5 with the Hectospec Multi-Object Spectrograph (MOS; Fabricant et al. 1998, 2005) on the 6.5 m MMT on Mt. Hopkins, as part of a larger program on massive stars in NGC 2403. The Hectospec[4] has a 1° FOV and uses 300 fibers each with a core diameter of 250 μm subtending 1.″5 on the sky. We used the 600 l/mm grating with the 4800 Å tilt yielding ≈2500 Å coverage with dispersion 0.54 Å/pixel and $R \sim 2000$. The same grating with a tilt of 6800 Å was used for the red spectra with ≈2500 Å coverage, 0.54 Å/pixel dispersion, and $R \sim 3600$. The total integration times were four hours and three hours, in the blue and red respectively. The spectra were reduced using an exportable version of the CfA/SAO SPECROAD package for Hectospec data.[5] The spectra were all bias subtracted, flatfielded, and wavelength calibrated.

A red spectrum of V12 (star 4 in Figure 1) was first observed with the MODS1 spectrograph on the Large Binocular Telescope (LBT) on 2014 January 6 with the 1.″0 wide long slit and the 670 l/mm grating yielding wavelength coverage from 5000 Å to 1 μm. V12 is very faint, $V \approx 23$ mag; consequently, the purpose of this observation was to obtain a moderately good S/N profile of its Hα line. The total integration time was 45 minutes. The spectra were bias subtracted and flatfielded using the MODS Spectral Reduction Package, and were then extracted, and wavelength and flux calibrated using the IRAF twodspec and onedspec packages.

When the MODS2 spectrograph became available in 2016, we obtained a second set of spectra using both spectrographs, one on each mirror, to observe red spectra with integration times of 90 minutes each, for a total of three hours yielding much better signal-to-noise. The spectra were observed on 2017 January 31. The seeing was excellent at 0.″6; consequently, the long slit was narrowed to 0.″6 yielding improved spatial and spectral resolution, $R \sim 2300$. The spectra were reduced as described above. They were wavelength calibrated using the night sky lines and flux calibrated with the standard star G191-B2B, observed immediately before V12.

2.2. Photometry

Previous images obtained with *HST* were used to derive magnitudes in our earlier papers on V37 (Van Dyk et al. 2006) and V12 (Van Dyk et al. 2005b). The new reduction package DOLPHOT (Dolphin 2000) has several advantages over DAOPHOT in these crowded fields. Consequently, we remeasured the images of V37 observed in 2004 with ACS/WFC and ACS/HRC, and the ACS/WFC images of V12 from 2004 using DOLPHOT. We have also reduced the more recent WFC3/UVIS and WFC3/IR images obtained in 2013 (GO-13477). The revised and new *HST* photometry in Table 1 for V37 and Table 2 for the four resolved stars in V12's environment are flight system Vega magnitudes. DOLPHOT uses the VEGAMAG zero points from Sirianni et al. (2005) for ACS/WFC and from the WFC3 web page,[6] for infinite aperture. Note that the new DOLPHOT photometry yields fainter magnitudes in all cases than the previously published data. The formal uncertainties reported by DOLPHOT for both WFC3 and ACS/WFC are quite good, 0.01–0.02 mag. The flight system magnitudes were transformed to the Johnson–Cousins system (*BVI*) using the conversion in Sirianni et al. (2005). These should be considered somewhat uncertain for stars with stellar winds. There is no current conversion of the WFC3 magnitudes to the Johnson–Cousins system, so *BVI* magnitudes are only available for 2004.

Spitzer/IRAC and MIPS observations of NGC 2403 were obtained as part of several different programs from 2004 to 2008. Here we combine the different data sets to derive improved fluxes for V12 and V37. We used the MOPEX (Makovoz & Khan 2005; Makovoz & Marleau 2005) package provided by the Spitzer Science Center to mosaic the individual artifact-corrected Basic Calibrated Data (cBCDs) and APEX Multi-Frame within MOPEX to perform point response function fitting photometry of point sources in NGC 2403. The detection threshold in MOPEX/APEX was set to 3σ in all bands. APEX detects a source near the SN 1954J position in IRAC channels 1 and 2 and at MIPS 24 microns, but not in IRAC channels 3 and 4. Similarly, no point source is detected at or near the SN 2002 kg position in any of the bands. We establish the upper limits to detection based on the fluxes of detected stars at or near the detection limit in the immediate environments of both SN 1954J and SN 2002 kg. The 24 micron region around V12 is complex with a variable

[4] http://www.cfa.harvard.edu/mmti/hectospec.html

[5] External SPECROAD was developed by Juan Cabanela for use on Linux or MacOS X systems outside of CfA. It is available online at http://iparrizar.mnstate.edu.

[6] http://www.stsci.edu/hst/wfc3/phot_zp_lbn

Table 1
Observed Colors and Luminosities for V37

Date	V	$B-V$	$U-B$	$V-R$	$V-I$	$E(B-V)$	V_0	$B-V_0$	$U-B_0$	$V-R_0$	$V-I_0$	M_v	Notes
1997 Oct 13	20.63	−0.08	−0.96	0.09	−0.06	0.19	20.09	−0.25	−1.09	−0.05	−0.34	−7.4	pre-max.
2001 Feb 20	20.65	0.27	⋯	⋯	−0.29	0.17	20.11	⋯	⋯	⋯	⋯	−7.4	pre-max
2003 Mar 26	18.32	0.13	⋯	0.28	0.35	⋯	17.78	−0.04	⋯	0.14	0.07	−9.8	near max.
2004 Aug 17[a]	19.43	0.21	⋯	⋯	0.21	⋯	18.89	0.04	⋯	⋯	−0.07	−8.6	post-max.

Note.
[a] Revised ACS/WFC photometry using DOLPHOT. Additional B- and R-band magnitudes were measured on 2004 September 21 with the ACS/HRC; $B = 19.54$, $R = 19.24$.

Table 2
Multicolor Photometry for the Four Stars in the V12 Environment

Star	F475W	F606W	F814W	F110W	F160W	B	V	I
2004 Aug 17 (ACS/WFC)								
1	24.22	22.59	20.86	⋯	⋯	24.96	23.10	20.87
2	24.22	22.60	20.99	⋯	⋯	24.96	23.10	21.00
3	23.09	23.06	23.04	⋯	⋯	23.08	23.06	23.04
4	24.11	23.23(23.32)[a]	22.73	⋯	⋯	24.50	23.44(23.52)[a]	22.72
2013 Oct 15 (WFC3)								
1	24.24	⋯	20.83	19.55	18.58	⋯	⋯	⋯
2	24.15	⋯	20.90	19.68	18.71	⋯	⋯	⋯
3	23.11	⋯	23.03	22.70	22.46	⋯	⋯	⋯
4	24.11	⋯	22.70	22.02	21.58	⋯	⋯	⋯

Note.
[a] Corrected for Hα.

Table 3
Spitzer/IRAC and MIPS Fluxes (μJy)

Star	3.6 μm	4.5 μm	5.8 μm	8.0 μm	24 μm
SN2002kg/V37	<17	<14	<10	<30	<750
SN1954J/V12	54.6 ± 0.4	33.2 ± 0.5	<147	<493	<2100 ± 15

background. We therefore also treat the measured flux as an upper limit. The array-location-dependent correction, the pixel phase correction, and color correction were all applied to the IRAC detections. The new fluxes are given in Table 3. Our measurements, while not identical, are consistent with those published by Kochanek et al. (2012).

3. V37(SN2002kg), an LBV/S Dor Variable

V37/SN2002kg was neither a supernova nor a giant eruption like SN1954J. It was discovered on 2003 October 22 (Schwarz & Li 2003), but first became visible a year earlier in images from 2002 October 26 obtained with the Katzman Automatic Imaging Telescope. It was initially classified as a Type IIn supernova (Filippenko & Chornock 2003) because of its narrow hydrogen emission lines. SN2002kg was later identified with the irregular blue variable V37 in NGC 2403 (Tammann & Sandage 1968) and shown to be an LBV/S Dor variable in eruption (Weis & Bomans 2005; Van Dyk et al. 2005b).

3.1. The Eruption and Post-eruption Spectra

Spectra observed during maximum light, 2003–2004, showed absorption lines characteristic of an early A-type supergiant (Maund et al. 2006; Van Dyk et al. 2006). Major

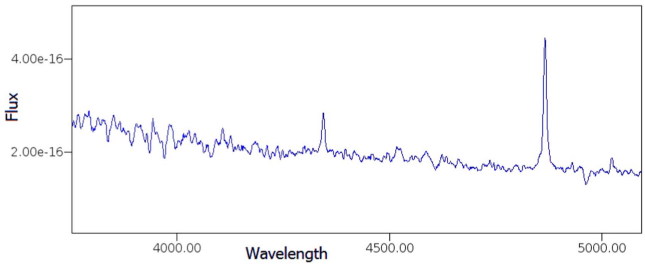

Figure 2. Flux calibrated (erg cm^{-2} s^{-1} A^{-1}) 2003 spectrum of SN2002kg (V37).

LBV outbursts usually develop strong F-type absorption-line spectra. This difference only means that V37's dense wind did not get as cool as recent examples such as Var C in M33 (Humphreys et al. 2014a) and R71 in the LMC (Mehner et al. 2013). Although, during its first recorded S Dor eruption in the 1970's, R71 also developed an A-type absorption-line spectrum (Wolf et al. 1981). Van Dyk et al. (2006) published four spectra and Maund et al. (2006) published two spectra covering the two year period from 2003 January to 2004 December. The spectrum from the MMT blue spectrograph observed on 2003 November 20 is shown in Figure 2. Strong absorption lines of hydrogen, Hϵ, λ3835 Å,

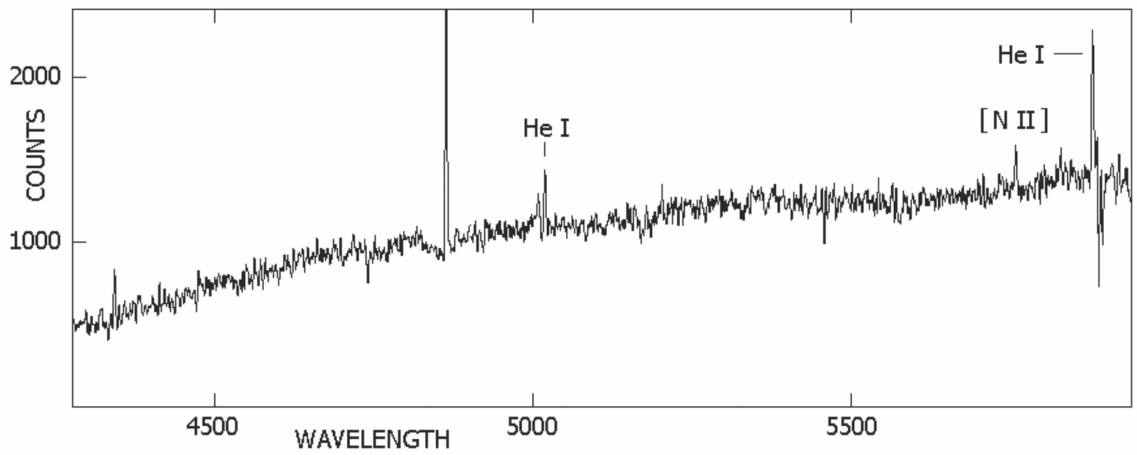

Figure 3. Blue spectrum of V37 from 2013. The He I λ5876 lines and the [N II] line at λ5755 are marked.

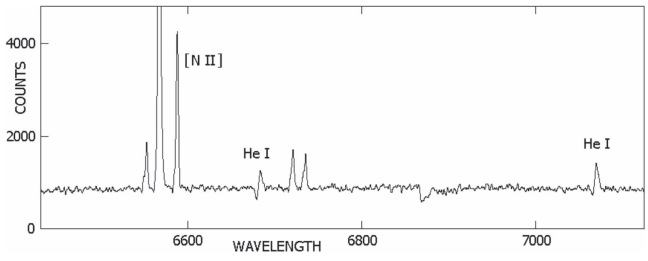

Figure 4. Red spectrum of V37 from 2013. The [N II] line at λ6584 and two He I lines with P Cygni profiles are marked.

and λ3889 Å, and the Ca II K line are conspicuous as are the hydrogen emission lines of Hα, Hβ, Hγ, and Hδ. Emission lines of Fe II and [Fe II] are also present. Although no P Cygni profiles are apparent, Thomson scattering wings common in strong stellar winds are observed on the hydrogen emission profiles.

The blue and red spectra of V37 from 2013 are shown in Figures 3 and 4. The star is quite faint and the spectra have low S/N. In addition to the hydrogen emission lines, the spectra show prominent P Cygni profiles in the He I emission lines at $\lambda\lambda$ 4471, 5015, 5876, 6678, and 7065 Å. The outflow or wind speed measured from the absorption minima in the P Cygni profiles in this low S/N spectrum is -187 ± 10 km s^{-1}. This velocity is consistent with the low wind speeds measured similarly for the LBVs in M31 and M33 by Humphreys. et al. (2014b) who reported that the winds of LBVs even in their quiescent state are slower than for normal hot supergiants.

The more recent post-eruption spectra also show the nebular emission lines of [N II] and [S II], and a relatively strong [N II] λ5755 line. The ratio of the [N II] lines $\lambda5755/\lambda6584$ indicates electron densities on the order of 10^6 cm^{-3}, greater than for an H II region. This suggests the presence of circumstellar nebulosity, which very likely formed during its 2002–2004 eruption.

3.2. The Luminosity before and during the Eruption

Pre-eruption photometry on the *UBVRI* photometric system (Van Dyk et al. 2006) is available from images obtained with the Nordic Optical Telescope on 1997 October 13 (Larsen & Richtler 1999) and on the $g'r'i'$ system from the Isaac Newton Telescope on 2001 February 20 (Maund et al. 2006, 2008). The pre-eruption magnitudes are summarized in Table 1. The interstellar reddening and visual extinction were independently derived from the two-color diagram (Van Dyk et al. 2006) and from stars within 2″ (Maund et al. 2006). Both approaches give approximately the same results with E_{B-V} of 0.19 mag and 0.17 mag, respectively (Table 1). Since the colors of luminous hot stars may be affected by emission lines, we adopt the reddening from the nearby stars ($A_V = 0.54$ mag), and using the Cardelli et al. (1989) extinction law we derive the intrinsic colors in Table 1. The 2001 B–V color (Maund et al. 2008) is much redder than the earlier photometry. Since those data were obtained only a short time before the eruption was detected, it is likely that V37 was already in transit to the cooler, maximum light state, although we would have expected the star to have begun to brighten in V. Maund et al. (2006) commented that the colors in their pre-eruption images were poorly constrained by the g′- and i′-band images. For that reason, we adopt the 1997 photometry and colors from the NOT for the pre-eruption star.

V37's pre-eruption intrinsic colors correspond to those of an early-type hot supergiant with an approximate spectral type of O9-B0. At a distance modulus of 27.5 mag (Freedman & Madore 1988) for NGC 2403, its M_V is -7.5 mag corrected for interstellar extinction. Adopting the corresponding bolometric correction (Flower 1996; Martins et al. 2005), the $M_{\rm Bol}$ of the pre-eruption star would be -10.4 mag. During its outburst, near maximum light, M_V was -9.8 mag from the 2003 March 26 photometry (Van Dyk et al. 2006) with the same A_V. The unreddened colors also correspond to a late B or early A-type supergiant consistent with the appearance of its spectrum during the eruption. With its corresponding bolometric correction, its luminosity was then $M_{\rm Bol} - 10.4$ mag near maximum. Based on stellar models with and without rotation (Ekström et al. 2012), V37's initial mass would have been 60–80 $M_\odot$.

Thus V37's outburst was like that of other LBV/S Dor variables, an apparent transit on the HRD, at nearly constant luminosity, due to increased mass loss and the formation of a cooler, dense wind. Also like other LBVs (Oksala et al. 2013; Humphreys. et al. 2014b; Kraus et al. 2014), V37 apparently did not form dust associated with its eruption (Kochanek et al. 2012), although it has apparently formed a post-eruption circumstellar nebula.

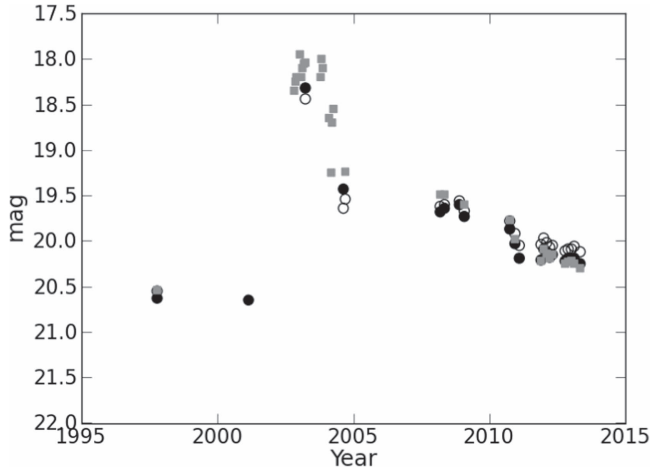

Figure 5. Light curve for V37, 1997–2013. Filled circles are the v-band magnitudes, open circles are b-band, and gray squares are r-band.

3.3. The Light Curve

V37's historical light curve can be seen in Tammann & Sandage (1968) and in Weis & Bomans (2005). We show V37's light curve from its current eruption in Figure 5 with the *V*- and *B*-band magnitudes from Table 1, the revised *B* magnitudes using DOLPHOT with the *HST*/ACS images from 2004, plus the R-band magnitudes from Van Dyk et al. (2006) to illustrate its maximum light. In addition, Kochanek et al. (2012) have published multicolor photometry from 2008 to 2011 from the LBT/LBC. The LBT/LBC photometry in poor seeing may have included light from a nearby star about 1 arcsec away (see their Figure 20). We therefore measured the brightness of this star in the ACS images and conclude that at ∼22 mag the fainter star does not contribute significantly to the magnitudes for V37. Their BVR band magnitudes are also included on Figure 5 plus additional LBT/LBC photometry from 2011 to 2013 (J. Gerke 2013, private communication). The post-eruption photometry shows that V37 was relatively constant from about 2004 to 2008 followed by a slow decrease until about 2010 when it began a more rapid decline.

4. V12 (SN1954J)—a Giant Eruption

V12 increased at least five magnitudes in apparent brightness during its eruption. Its historical light curve showing its 1954 eruption (Tammann & Sandage 1968) is reproduced in Figure 6. Its pre-eruption light curve is remarkable for the rapid variations in its apparent magnitude in the years 1950–1954 prior to its giant eruption, sometimes a half magnitude or more in only a few days. These erratic fluctuations are most likely due to a short-term surface instability distinct from the LBV/S Dor long-term eruptions, which have different characteristics. η Car also displayed rapid oscillations prior to its "great eruption" in 1843. Similar variability was also reported in the pre-outburst light curve of the SN impostor UGC 2773-OT (Smith et al. 2010), and multiple outbursts have been observed in the impostor SN 2000ch (Wagner et al. 2004; Pastorello et al. 2010) as well as SN 2009ip before its presumed terminal explosion (Mauerhan et al. 2013a; Pastorello et al. 2013; Margutti et al. 2014). These geyser-like lesser outbursts may be clues to the cause of the

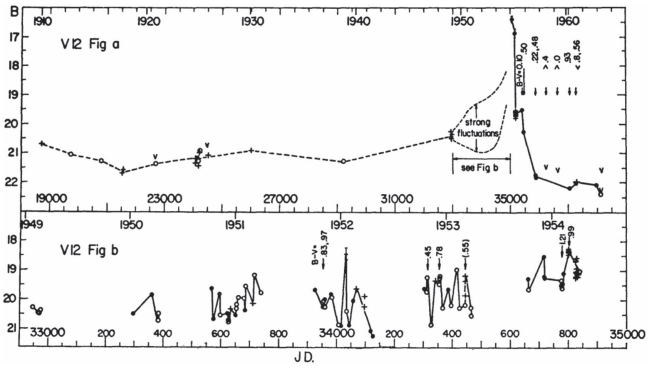

Figure 6. Historical light curve for V12 (SN1954J) from Tammann & Sandage (1968).

giant eruption, although the origin of these instabilities is likewise not understood.

These short-term variations in V12 were superposed on a rather slow increase in brightness from about 20.5 mag in late 1949 to 19.1 mag in 1954 March. There is then a seven month gap in its photometric record because of its proximity to the Sun at the time. When next observed in 1954 November, it was at apparent *B* magnitude 16.46, after which it rapidly declined with an apparent short plateau or shoulder on its light curve that lasted another seven months.[7] A short shoulder on the declining light curve is also observed in the light curves of other giant eruptions including P Cyg, SN1961V, and probably η Car (Humphreys. et al. 1999). Mauerhan et al. (2013b) have suggested that these plateaus, which look like a brief stall in the declining light curve, are due to the interaction of the expelled mass with previously ejected circumstellar material. If correct, this is evidence that V12 may have had previous high mass-loss events.

Unfortunately, we do not know its luminosity at maximum. Based on the observed magnitudes, V12 reached an absolute *B* magnitude of at least $M_B = -11.0$. Correcting for possible interstellar extinction of $A_V \approx 0.9$ mag (1.2 mag A_B), based on the discussion in Section 4.2, $M_{\rm Bmax}$ would be at least −12.2 mag. Although no color was recorded at maximum light, its color, reported several times during its rise (1951–1954), was $B - V \simeq 1.0$, consistent with the production of a cool, dense wind with a negligible bolometric correction. Adopting this color, and correcting for extinction, then $M_V \approxeq M_{\rm Bol}$ at maximum was −12.9 mag, or greater; comparable to several other SN impostors with reported maximum luminosities on the order of −13 to −14 mag.

[7] The apparent plateau corresponds to a second gap in the observations when NGC 2403 was not observed due to its position on the sky. On 1955 March 29–30 and on 1955 October 21–22, V12 was measured at 19.6 and 19.5 mag, respectively, hence the conclusion that it had not varied significantly during that time. The magnitudes from Tammann & Sandage (1968) were measured from photographic plates and there is always some question about the associated errors or uncertainties. Tammann & Sandage (1968) used a primary photoelectric sequence on the photographic plates. Based on their discussion, the error for the sequence stars brighter than 19.5 mag is ±0.02 mag. For stars fainter than 21 in *B*, it is ≈±0.1 mag. Another way to estimate the likely error specifically for V12, is to compare measurements separated by only a few days when it was not varying rapidly. We find a scatter typically ±0.05–0.10 mag in *B* when it was a 21st mag star, and ±0.10 mag in *V* from their Tables A3 and A4, respectively, which supports internal consistency.

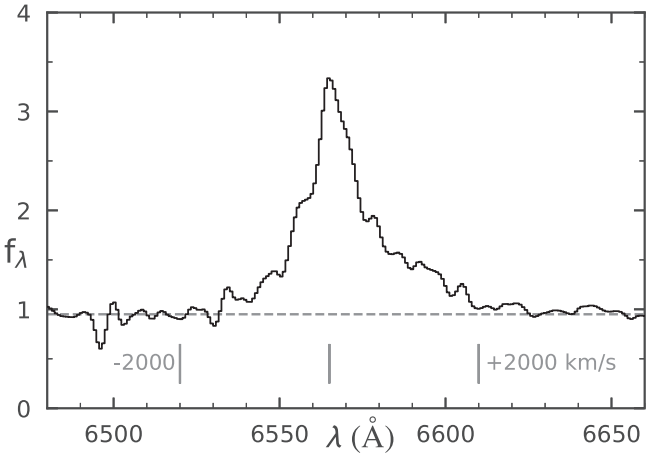

Figure 7. Flux calibrated Hα profile of V12 in 2017 January. The units for f_λ are 10^{-17} erg cm^{-2} s^{-1} A^{-1}.

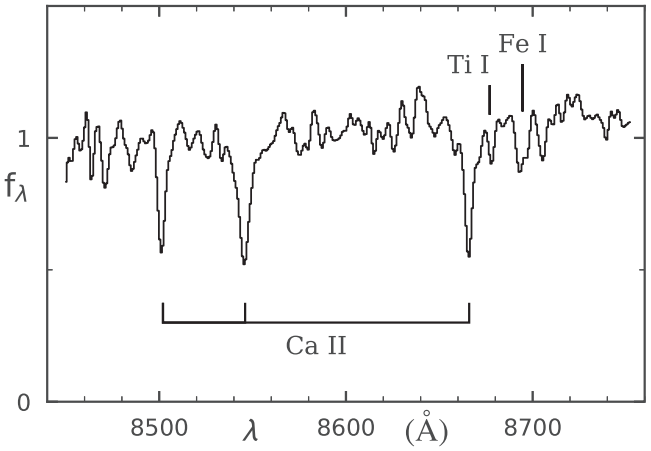

Figure 8. Ca II triplet in V12. The absorption lines of Ti I (λ8675 Å) and Fe I (λ8688 Å) are also identified. The units are 10^{-17} erg cm^{-2} s^{-1} A^{-1}.

4.1. The Post-eruption Spectrum—Hα and Absorption Lines

The Hα emission profile from our 2017 January LBT/MODS1+MODS2 spectrum of star 4 is shown in Figure 7. This is the line profile of a stellar wind, not a supernova remnant. It has broad asymmetric wings characteristic of Thomson scattering, unrelated to bulk motion of the gas, and there is no obvious P Cygni absorption feature. The line profile's total equivalent width is 59 Å and its net flux corrected for interstellar extinction (Section 4.2) is 1.1×10^{-15} erg cm^{-2} s^{-1} (1.1×10^{-18} W m^{-2}), about 330 $L_\odot$ at the distance of NGC 2403. There is no significant change in the flux from the 2014 spectrum. Its FWHM line width of 13.5 Å corresponds to a velocity of 620 km s^{-1} similar to η Car's value of 600 km s^{-1}. This may be an overestimate because the profile is already asymmetric at the half maximum level (2.17×10^{-17} erg cm^{-2} s^{-1}). Before the profile begins to noticeably broaden, the width is about half that, equivalent to 270 km s^{-1}, measured at 2.84×10^{-17} erg cm^{-2} s^{-1}. The asymmetric wings extend to −1530 km s^{-1} and +2000 km s^{-1}. The heliocentric velocity of the peak of the Hα line is 133 km s^{-1}.

The red spectrum also reveals several absorption lines shown in Figure 8. The near-infrared Ca II triplet is readily identified. The lack of emission and P Cygni profiles in the Ca II lines, often seen in the spectra of cool stars with high mass loss and circumstellar ejecta (Humphreys et al. 2013; Gordon et al. 2016), is somewhat surprising. Several other absorption lines of Fe I, Ti I the Mg I triplet at λ8806 Å, and the Si I doublet at ≈8751 Å are also present. These neutral metallic lines imply that the photosphere or very dense wind is relatively cool, corresponding to a star later than spectral type F. The lack of a strong O I λ7774 line also requires a later spectral type. We use the Ca II spectral library (Cenarro et al. 2001)[8] to estimate a mid- to late-G spectral type based primarily on the strength of the Ca II lines and the neutral lines. The Fe I and Ti I lines all show increasing strength with luminosity. The line ratio Fe I λ8688 to Ti I λ8675 is a known luminosity indicator (Keenan & Hyneks 1945). Our measured ratio, 1.5–1.9, for this line pair in V12 compared with ratios of 1.3 to 2.0 measured in several G-type supergiants in the spectral library suggests a relatively high luminosity for the G-type star. We also note that the equivalent width of the luminosity sensitive O I λ7774 line is the same as that measured in a G5 supergiant in M31 (Gordon et al. 2016). Based on its spectral characteristics, we would expect an apparent temperature of ∼5000 K. The average heliocentric velocity of the Ca II lines is 138 ± 1 km s^{-1} compared with 133 km s^{-1} for the Hα peak. The systemic velocity of NGC 2403 is 133 km s^{-1}. V12 is located very close to the minor axis of the galaxy and only ≈1.5 kpc from the center so it is not surprising that the measured velocities are close to the systemic.

4.2. Interstellar Extinction and the Spectral Energy Distribution

HST imaging resolves V12 into four stars (Figure 1). The strong Hα source, star 4, is the most likely candidate for the surviving star. The *HST*-based VEGAMAGS in Table 2, separated by nine years, also shows that none of the four stars have varied significantly in the past decade. Assuming that these stars are also members of NGC 2403, they make up the immediate environment of V12 and can be used to estimate the internal interstellar extinction. Van Dyk et al. (2005b) discussed the two-color *B–V* versus *V–I* diagram using their earlier DAOPHOT photometry, and concluded that star 3 is most likely a reddened hot star and the two redder stars are red supergiants.

We use the revised magnitudes from DOLPHOT for the 2004 ACS data for the two-color diagram (F475W-F606W versus F606W-F814W), in Figure 9. It does not look much different from their earlier figure except that the errors are much smaller with DOLPHOT. The smooth curve is the intrinsic color locus for supergiants based on the Castelli–Kurucz models (Castelli & Kurucz 2004), convolved with the ACS/WFC filter functions using STSDAS/SYNPHOT. The dotted line from the tip (hottest) of the supergiant locus is the reddening vector for $A_V = 1.0$ mag using the Cardelli et al. (1989) interstellar extinction curve. Star 4 lies blueward of the intrinsic color curve. Indeed its colors are anomalous; it is too blue for its apparent G spectral type. Star 3 lies close to the intrinsic color line. Its colors suggest a hot star with $A_V \approx 0.9$ mag., or alternatively an intermediate temperature star (B8 I-A0 I) with only the Galactic foreground extinction of 0.11 mag (Schlafly & Finkbeiner 2011), and therefore virtually no internal interstellar extinction from NGC 2403. But the colors of the two red supergiants also indicate some additional internal

[8] http://pendientedemigracion.ucm.es/info/Astrof/ellipt/CATRIPLET.html

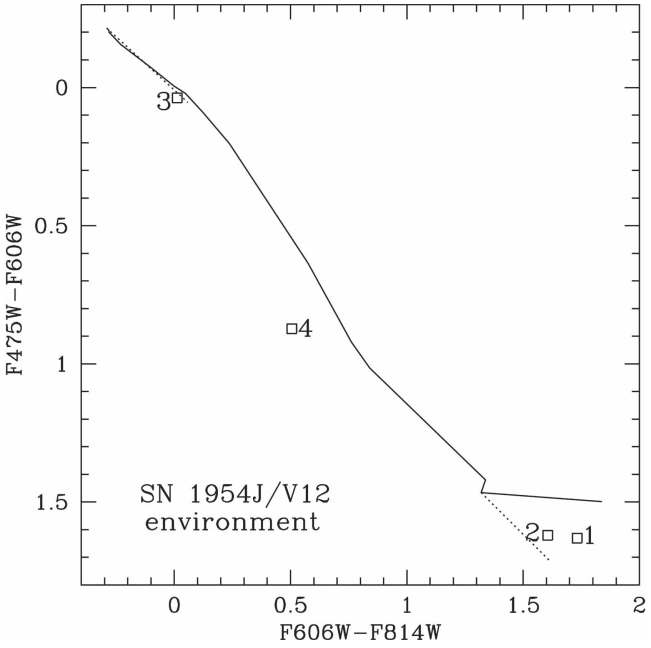

Figure 9. Two-color diagram for the four stars in the V12 environment using the VEGAMAGS from 2004.

extinction; they would lie on the intrinsic color with an A_V of ≈0.8 mag. Given V12's location in an association of young stars in a spiral arm, some internal reddening is expected. For example, V37 discussed previously has an A_V of 0.54 mag. Our results suggest an A_V of 0.8–0.9 mag for the V12 environment.

Using the *BVI* magnitudes in Table 2 with A_V of 0.9, star 4 has a current M_v of −5.0 mag with an intrinsic $B - V \approx 0.76$ mag., suggestive of an intermediate temperature star with a corresponding $M_{\rm Bol}$ of −5.1 mag, only $\sim 8 \times 10^3\, L_\odot$. The derived intrinsic color suggests a mid F-type star, which is not supported by the absorption-line spectrum. The expected intrinsic $B - V$ color for a mid- to late-type G supergiant is 0.9–1.0 mag. The derived luminosity is also discrepant with the luminosity indicators in its spectrum. This relatively low luminosity would place star 4 well below the AGB limit on the HRD.

Star 4's current spectral energy distribution (SED) is shown in Figure 10 together with the SEDs for the two red stars combined and for star 3 for comparison. We use the fluxes for the flight system[9] magnitudes in Table 2. The observed magnitudes are corrected for the adopted interstellar extinction using the Cardelli et al. (1989) extinction curve. The contribution from the Hα line has been removed from the F606W flux for star 4. The *Spitzer*/IRAC and MIPS measurements from Table 3 will include the light from all four stars and are therefore shown on all three SEDs. They reveal a near-infrared source at 3.6 μm and 4.5 μm, upper limits at 5.8 μm and 8.0 μm, and an upper limit on a mid-infrared source at 24 μm from MIPS.

Planck curve fits are shown for all three SEDs. For the purposes of this paper, the Planck curve adequately approximates the continuum at blue to far-red wavelengths—i.e., the

[9] We use the Vega flux calibration for the ACS/WFC and WFC3 filters at http://www.stsci.edu/hst/acs/analysis/zeropoints/# vega and at http://www.stsci.edu/hst/wfc3/phot_zp_lbn with the pivot wavelengths of the filters.

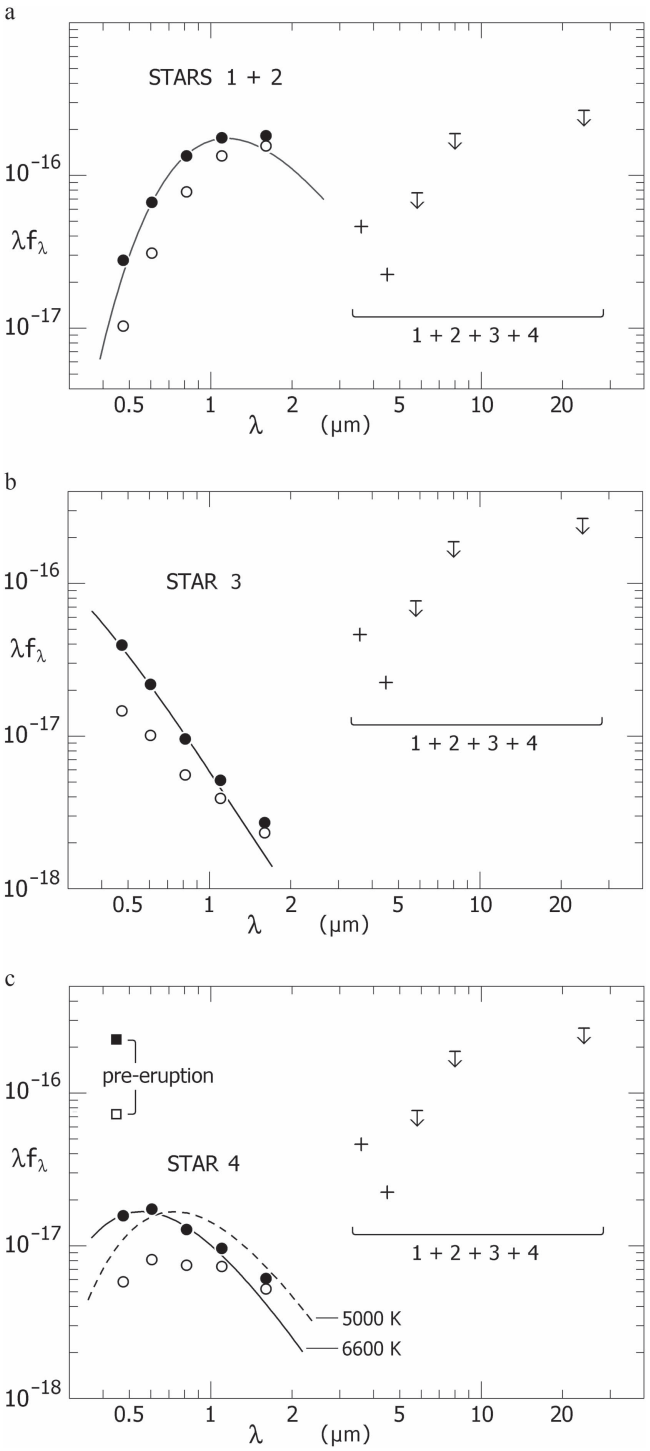

Figure 10. (a) The combined SED for the two red stars. A 3200 K Planck curve is shown for their extinction-corrected combined fluxes. Open circles are the observed fluxes based on VEGAMAGs and the filled circles are corrected for interstellar extinction, $A_V = 0.8$ mag. These two red stars are the probable sources of near-IR flux at the position of V12. Units for λf_λ are W m^{-2}. (b) The SED for star 3. Open circles are observed fluxes based on VEGAMAGs, and filled circles are corrrected for interstellar extinction, $A_V = 0.9$ mag. A 25,000 K Planck curve is shown. λf_λ is expressed in W m^{-2}. (c) The SED for star 4. Observed fluxes from VEGAMAGs are shown as open circles, and filled circles are corrected for interstellar extinction $A_V = 0.9$ mag. The best-fit Planck curve has $T = 6600$ K, but the absorption-line spectrum indicates 5000 K. The pre-eruption magnitude in 1910–1938 is also shown. Units for λf_λ are W m^{-2}.

temperatures are meaningful even though they differ a little from the formal effective temperature $T_{\rm eff}$.[10]

The two red stars have nearly identical magnitudes and colors and are clearly the dominant contributors to the near-IR flux as illustrated by their combined SED (Figure 10(a)). Star 3 is a hot supergiant. The Planck curve suggests a temperature of 15,000 to 20,000 K with a small free–free excess (Figure 10(b)). The best Planck curve fit to star 4 (Figure 10(c)), however, indicates a much warmer temperature, ∼6600 K, corresponding to a mid F-type supergiant, than indicated by the absorption lines. A 5000 K blackbody is shown for comparison as are the magnitudes for the pre-eruption star. The likelihood that star 4 is actually two stars is discussed more thoroughly in Section 4.4.

4.3. The Nature of the Progenitor

V12's historical light curve (Figure 6) shows that the progenitor was significantly brighter than the apparent survivor is today. Prior to its erratic rise to maximum, V12 had an average pre-eruption (1910–1938) photographic or B magnitude of 21.2 mag from the F(air) and G(ood) quality magnitudes from Table A3 in Tammann & Sandage (1968). These photographic magnitudes refer to the integrated light of the four stars resolved by *HST*. Today, the combined apparent B magnitude of the four stars in Table 2 is 22.55 mag, 1.3 mag fainter than in its pre-eruption state. Assuming that the other three stars had the same blue magnitudes they have today, then star 4 would have had to be a 21.5 magnitude star prior to the eruption, 2.5 to 3 magnitudes brighter than its current blue magnitude. Adopting A_V of 0.9 mag (A_B of 1.2 mag), its absolute blue magnitude then was −7.2. Assuming the $B-V \cong 1.0$ mag color observed frequently during the rise to maximum, its M_V would be −7.9 mag and with no bolometric correction, the progenitor would be an intermediate temperature supergiant with a luminosity of $\sim 10^5\,L_\odot$ and an initial mass of $\sim 20\,M_\odot$. Of course if the star was hotter, it would be more luminous.

Thus the likely survivor, star 4, is now approximately 2.5 to 3 mag fainter than its probable progenitor, and its luminosity today is at least 10 times fainter. This is a surprising result. As the star recovers from a giant eruption, it is expected to restore hydrostatic and thermal equilibrium. We therefore expect the star to return to close to its pre-eruption luminosity. η Car is the best example we have of a star recovering from a giant eruption, and the data on its pre-eruption state support very little or no change in its total luminosity (Davidson & Humphreys 1997).

Some may argue that there is no problem; the SN1954J eruption was terminal, i.e., a true supernova, the star is gone, and the object we now observe is a completely different star. However, 60 years later, there is no evidence for an SN remnant at the position of star 4. There is no X-ray source (Binder et al. 2015) or nonthermal radio source (Eck et al. 2002) at or near its position, and the Hα profile is representative of a stellar wind.

Another possibility is that star 4 is actually more than one star. Star 4 in the F658N image has a Moffat FWHM of 1.47 pixel, while both stars 1 and 2, interestingly, have FWHM of 2.12 and 2.01, respectively. The PSF for star 4 is consistent with what would be considered stellar, or at least, unresolved. The corresponding region sampled with ACS/WFC is only 1.1 pc at the distance of N2403. Of course, this does not rule out the presence of another star in the PSF. As already mentioned, star 4's colors are too blue for the G spectral type. V12 could also be a binary or a multiple system, but that would not solve the problem of the decrease in apparent brightness and luminosity. Possible models for star 4 are discussed below.

4.4. Conceptual Models for Star 4

It is surprisingly difficult to assemble a model that explains all the data on V12. The Hα emission line, for instance, causes trouble in the following way. Its profile (Figure 7) has the classic shape produced by Thomson scattering in a mass outflow, with asymmetric quasi-exponential wings extending to −1500 and +2000 km s^{-1}—see, e.g., Auer & Van Blerkom (1972), Davidson et al. (1995), Dessart et al. (2009), and Humphreys. et al. (2012). The long-wavelength wing appears consistent with average optical depth $\tau_{\rm sc} \gtrsim 1$ in the Hα emission region. Since line profiles of this type characteristically occur in giant eruptions and other very dense outflows, this interpretation seems natural for V12—but the simplest models predict inadequate values of $\tau_{\rm sc}$. Below we sketch the most evident possibilities for star 4.

1. Suppose that this object is currently a supergiant with $L \gtrsim 10^4\,L_\odot$, $T_{\rm eff} \approx 5000$ K, and $R \gtrsim 130\,R_\odot$. The temperature is indicated by the Ca II triplet and other absorption features (Section 4.1). But the SED shown in Figure 10(c) requires $T \approx 6600$ K, a temperature difference that is spectroscopically unacceptable. Moreover, a single-supergiant model fails to explain the Hα profile. In order to produce the observed Hα luminosity in an envelope or wind around such a large star, the ionized density just outside radius R must be of the order of $n_{\rm e} \sim 10^{10}$ cm^{-3}. The resulting optical thickness for Thomson scattering is only $\tau_{\rm sc} \sim 0.1$, which is too small to create the Hα line wings. This difficulty is basically a consequence of the star's large radius. The discrepancy worsens if we allow for inhomogeneous densities, and circumstellar extinction (Section 4.6) would not help. Hence, in this model, the Hα line shape must be caused by an unusual distribution of bulk outflow velocities, with a maximum that is much larger than the escape velocity (roughly 2000 km s^{-1} versus 200 km s^{-1} respectively). In summary, this object appears more complicated than a single G supergiant.
2. The most obvious possibility is to add another, hotter star. There is nothing implausible about either a binary companion, or an unrelated object within about 1 pc. As already emphasized, star 4's SED cannot be fit by a single 5000 K star. The observed spectrum sets limits on the hypothetical second object. The lack of He I emission (λ5876 and λ6678) in a star with a strong stellar wind suggests that it is not likely to be much hotter than 20,000 K, while a 7000–10,000 K object would contribute features not observed in the red spectrum. A combination of two stars can account for both the blue-to-red SED and the Ca II triplet near 8500 Å. Figure 11 shows an example with temperatures of 5000 K and 20,000 K; note that the cooler object must dominate around 0.85 μm so Ca II can

[10] Elaborate photosphere models would require more parameters than our data can support, and, besides, are beyond the scope of this paper. For $\lambda \lesssim 0.37$ μm, the Balmer discontinuity may indirectly cause our blue-to-red Planck-fit temperatures to exceed the true $T_{\rm eff}$, but this effect is not large for supergiants, and the Paschen jump is smaller. At $\lambda \gtrsim 0.8$ μm, free–free emission from a stellar envelope or wind may supplement the continuum.

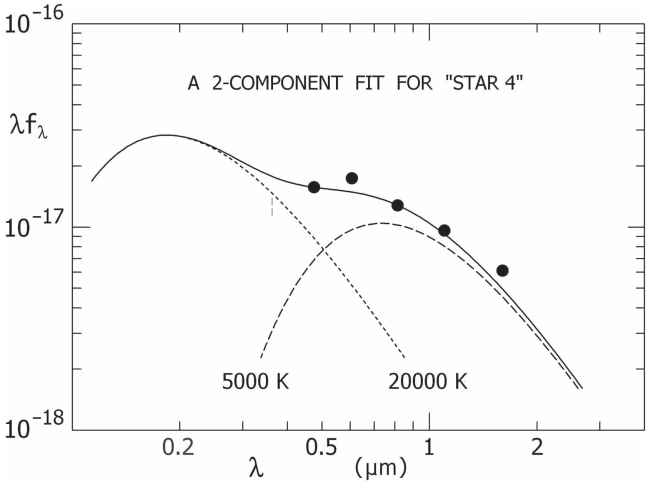

Figure 11. Typical two-component fit to the SED for star 4 with a 5000 K Planck curve inferred from the G-type absorption lines and a hotter 20,000 K star as discussed in Sections 4.4 and 4.6. A small vertical mark indicates the Balmer discontinuity wavelength. Possible circumstellar extinction is not included.

be prominent. The giant eruption survivor is presumably the hotter object, because it can have an unusually dense wind to account for the brightness and profile of the Hα emission. Since it is much smaller than the G supergiant, its wind can have $\tau_{sc} \sim 1$ while producing the right amount of Hα. Incidentally, there is no need to postulate a close *interacting* binary. More details are outlined in Section 4.6 below.

3. Other scenarios are more complicated. For instance, the Hα might originate in ejecta from the 1954 eruption, now located at $r \sim 4000$ to 8000 au assuming expansion velocities of 300–600 km s^{-1} based on the width of the Hα line. Such models can be devised for ejecta masses in the range of 0.1 to 10 $M_{\odot}$, with suitable densities and volume filling factors. Thomson scattering is then negligible, so the Hα profile must represent line-of-sight bulk expansion velocities. This is unsatisfying, because it does not account for the Ca II versus SED mismatch noted above, and also because the ejecta velocity distribution fortuitously mimics a Thomson-scattered profile. The observed asymmetry in the profile (red side brighter) matches Thomson scattering but is opposite to what one normally expects for a Doppler profile in expanding ejecta.
4. Perhaps SN 1954J was a genuine supernova event, and the bluer SED plus Hα emission are associated with a resulting neutron star or black hole near the G-type supergiant. If we speculate that the pre-1954 state was a close binary, then the unusual faintness of the SN event might be ascribed to the exploding star's small size, i.e., maybe it had transferred most of its mass to the G supergiant. In some respects this is an appealing scenario, but there are serious objections. (a) The hypothetical accreting neutron star of the black hole should probably be an X-ray source, but none have been detected (Binder et al. 2015). (b) The supergiant should very likely have an anomalously high velocity of the order of 40 km s^{-1}, due to its pre-event orbit, but this is not evident in the spectra. (c) This model does not account for the Hα line shape. The asymmetry of a classic Thomson-scattered profile results from expansion of the gas, unlike an accretion flow toward a compact object. Thomson scattering would indeed be effective in such a compact Hα source, but it would produce a different line shape. (d) We do not have a model to explain why the accretion disk or inflow produces a bright continuum at the blue-visual wavelengths.
5. Suppose that there is only one star, but Ca II and other absorption lines are formed in outer, cool zones of a dense wind, rather than a normal photosphere. Such an outflow would be unsurprising, given the precedent of η Car in the state that was seen 60 years after its giant eruption (Humphreys et al. 2008). Standard spectral classification criteria are not valid for dense winds (Davidson & Humphreys 2012; Davidson 2016), so the star can be hotter and smaller than the 5000 K supergiant deduced in Section 4.1. The continuum may even originate in a diffuse opaque-outflow photosphere (Davidson 1987, 2016; Owocki & Shaviv 2016), rather than a static stellar photosphere. Unfortunately, the dense-outflow idea cannot by itself overcome the Hα objection in point 1 above; with any credible cool photosphere radius, say $R > 50\,R_{\odot}$, one finds $\tau_{sc} \lesssim 0.3$ in a spherical region that produces the observed amount of Hα emission. Perhaps $\tau_{sc} \sim 1$ can be attained with a more localized emission volume—e.g., in a bipolar flow—but this possibility is quantitatively marginal. Moreover, one would expect the Ca II absorption to be blueshifted relative to the Hα peak, contrary to the data. In summary, this model avoids the need for a second component and it cannot be dismissed, but it appears less successful than model 2 above.

None of the above scenarios are entirely satisfactory, but in our opinion model 2 is by far the simplest and most likely. Except for the possible supernova binary model, none of them alone can explain the decline in apparent luminosity from $10^5\,L_{\odot}$ before the eruption to $10^4\,L_{\odot}$ afterward. Furthermore, even in the SN model, luminosity indicators in the spectrum of the G-type star do not match its current state. The most likely explanation for this luminosity discrepancy is post-eruption dust formation and circumstellar extinction, see Sections 4.5 and 4.6 below.

In the next section, we examine the possibility of dust formation, and the limits set by the mid-infrared flux shown in the SEDs.

4.5. Circumstellar Dust, Extinction, and Mass Loss

The historical light curve shows some evidence in support of dust formation. After maximum light, the apparent brightness rapidly declined at blue wavelengths. By early 1957, it was fainter than the pre-eruption state, and post-eruption magnitudes from 1957 to 1963 progressively faded from 21.75 to 22.4 mag. The few color values also show that it was becoming redder, consistent with increasing circumstellar extinction. The faintest blue magnitude recorded in those years was 22.4, interestingly close to what we observe today. Of course those measurements referred to the sum of all four objects, but evidently one of them—almost certainly star 4—became fainter than it had been a few decades earlier, and dust formation is arguably the simplest explanation. Indeed it may have faded even more after 1963, followed by partial brightening in recent years as the dust moves outward. In this section, we outline the implications of dust formation in this object, an unsettled topic.

Possible circumstellar dust associated with V12 has been discussed by several authors, without agreement. Smith et al. (2001) suggested that V12 had a near-IR excess due to dust, based on groundbased UBVRIJHK photometry that included all 4 stars. Van Dyk et al. (2005b) based their arguments for dusty ejecta on the Hα line, presumably indicating a luminous hot star, together with star 4's location in their two-color diagram. They suggested a combined $A_V \approx 4$ mag, interstellar plus circumstellar extinction. In contrast, Kochanek et al. (2012) disputed this conclusion, arguing that the mid-infrared fluxes from *Spitzer* and obscuration could not come from the low luminosity and temperature that they estimate for star 4. The *Spitzer*/IRAC and MIPS fluxes represent the integrated light of all four stars including the two red supergiants. Our improved *HST* photometry permits an assessment of the four objects' relative contributions.

If the ejecta from V12's giant eruption did produce dust, it should now be at $r \gtrsim 4000$ au with expansion speeds of 300–600 km s^{-1}. Assuming a luminosity of $10^5\ L_\odot$ for the progenitor, with efficiencies $Q_\lambda \approx 0.03$ to 0.1 for reradiation by dust, the dust temperature should be 130–180 K with peak radiation near $\lambda \sim 16$–22 μm. If the expansion was faster, the dust may be further from the star, cooler and radiating at longer wavelengths. The *Spitzer*/MIPS flux in the 24 μm band shows a mid-infrared source, but, given the complexity of the region and background at such wavelengths, we consider that measurement to be an upper limit for V12. With 6″ resolution and 2.″5 per pixel, it refers to the combined light of all four stars like the other infrared data.

We can reasonably expect that hot star 3 does not make a significant contribution at this wavelength. The two red supergiants, however, may make appreciable contributions from silicate emission around 24 μm. They appear nearly identical in the photometry. Using our measurement of the interstellar extinction, each has $M_v \approx -5.2$ and their intrinsic colors suggest an early M spectral type. The corresponding bolometric luminosities are −6.4 mag. To estimate their likely contribution to the 24 μm flux, we selected four M supergiants in the Per OB1 association ($D \approx 2.2$ kpc) with *ISO* spectra and comparable luminosities and spectral types. Their average flux at 24 μm is 14 Jy, which scaled to the distance of NGC 2403 becomes 7.4×10^{-6} Jy. Since this is far below the measured flux for V12, the two red supergiants therefore do not account for it. Although PAH emission dominates in the 8 μm band, the radiation at 24 μm is mostly thermal emission from grains with temperatures $\gtrsim$100 K. We therefore suggest that much of the mid-infrared flux in the V12 environment comes from ejecta associated with star 4.

We can use the flux at 24 μm to estimate limits on the mass of the dusty circumstellar material and the total mass lost in the giant eruption. The dust mass is given by

$$M_{\rm dust} = \frac{4D^2 \rho \lambda F_\lambda}{3(\lambda Q_\lambda / a) B_\lambda(T)},$$

where D is the distance to NGC 2403, F_λ is the flux, a is the grain radius, $\rho \approx 3$ g cm^{-3} is the grain density for silicates, Q_λ is the grain efficiency for the absorption and emission of radiation, and $B_\lambda(T)$ is the Planck specific intensity at temperature T. For this calculation, we adopt a dust temperature of 150 K and $a = 0.5$ μm. Using the formulation from Suh (1999), $Q_\lambda \approx 0.035$ at 21–26 μm. The upper limit to the mass in dust is then 2×10^{31} g. Assuming the conventional gas to dust ratio of 100, this suggests that the ejected mass is on the order of 0.5 $M_\odot$. Hence the average rate as V12 faded in 10 years was $\approx$0.05 $M_\odot$ yr^{-1}. Presumably the rate during the event was much higher, and perhaps unsteady. If some of the dust is at large optical depths, i.e., shielded from most of the star's light, then it may be cool and thus excluded from the above estimate. There also may have been additional mass loss during V12's erratic short-term outbursts prior to maximum.

If circumstellar dust absorbs most of the light from star 4, then the 24 μm data may constrain the total luminosity. The reasoning, however, is far from robust. If some of the 24 μm flux comes from unrelated dust in a larger region, then this method overestimates the amount of light from star 4; or, on the other hand, if some of the light escapes through gaps in the dust shell, then we get an underestimate. Moreover, we know very little about the grain properties, and η Car's unusual grains serve as a cautionary example regarding eruptions (Davidson & Humphreys 1997). Nevertheless, we adopt simplified assumptions here to estimate the dust luminosity. If the grain radiative efficiency has wavelength dependence $Q_{\rm abs} \propto \lambda^{-2}$ in the mid-infrared, and the 24 μm flux approximates the peak of the λf_λ curve, then the grain temperature is about 100 K. In that case, the observed $\lambda F_\lambda \approx 2.6 \times 10^{-16}$ W m^{-2} implies a total flux $F_{\rm IR} \approx 4 \times 10^{-16}$ W m^{-2} and $L_{\rm IR} \approx 10^5\ L_\odot$ at NGC 2403.[11] If instead the dust temperature is 150 K, then the peak $L_{\rm IR}$ is 50% larger. If $Q_{\rm abs} \propto \lambda^{-1}$, then the optimum grain temperature is about 120 K instead of 100 K and $L_{\rm IR}$ is about 10% above the other estimates. In addition, the 8 μm upper limit implies that $L_{\rm IR}$ cannot be larger than about twice the quoted limit. Allowing for some of the uncertainties, $L \sim 2 \times 10^5\ L_\odot$ appears to be a credible upper limit—except that the reasoning becomes invalid if a substantial fraction of the light escapes through gaps in the dust shell.

Circumstellar dust can evidently account for most of the apparent post-eruption decrease in the brightness noted above. Star 4's current luminosity corrected for interstellar (not circumstellar) extinction is roughly $10^4\ L_\odot$. The various quantities appear to permit a circumstellar extinction factor of the order of 10, thereby allowing a corrected $L \sim 10^5\ L_\odot$, which one informally expects for a giant eruption survivor. This question is discussed further in Section 4.6 below.

Extinction of the order of two magnitudes normally implies conspicuous reddening, but this depends on grain properties, which can be peculiar in a giant eruption or massive stellar wind. Anomalous extinction is well documented for, e.g., stars in the Carina Nebula (Thé & Graaland 1995). The extinction/reddening ratio A_V / E_{B-V} ranges from a normal value near 3 to a high of 6, and probably higher for η Car. In other words, strong extinction does not always imply strong reddening. Anomalous extinction curves of this type are attributed to large grain sizes, and play a role in the next subsection.

4.6. A Quantitative Model with Circumstellar Reddening

As noted above, two strong clues imply the presence of circumstellar extinction for star 4 (which is two objects). First, if we apply only the interstellar correction used in Figures 10(c) and 11, the 5000 K supergiant at 0.8 μm appears to have $L \sim 4000$ to $8000\ L_\odot$ or $M_{\rm bol} \approx -4.6$ to −5. But the luminosity indicators in its spectrum imply a much higher

[11] Here we include a 30% allowance for the fact that the dust SED is broader than the Planck function, since it includes a range of temperatures.

luminosity (Section 4.1), thus requiring an additional extinction correction of roughly 2 to 3 mag at $\mu \approx 0.8\ \mu$m. Second, note the pre-eruption brightness indicated in the upper-left part of Figure 10(c). As explained in Section 4.2, it represents only star 4, the others being subtracted out. The present-day star 4 appears fainter by roughly 2.8 mag in the "*B*" band. Thus, if it is in the same state as in 1910–1938, we need that amount of additional extinction near $\lambda \approx 0.45\ \mu$m. (Later we mention physical reasons why the eruption may have caused a decrease in brightness at blue wavelengths, but they cannot explain a factor larger than about 0.8 mag.) We assume that the circumstellar extinction equally affects the hot component, and the G supergiant, and the Hα emission; otherwise, a self-consistent model becomes more difficult.

The above clues favor circumstellar extinction with $A_V \sim 2.5$ and only weak reddening, $A_B - A_V < 0.5$. Moreover, stronger reddening would almost preclude a consistent two-star model. In such a case, the hotter star is found to dominate at all wavelengths, making it impossible for the Ca II triplet and the other neutral lines to be as strong as they are in the combined spectrum (Figure 8). Hence there are two independent reasons to suppose that the reddening is weak. This is quite reasonable, since large extinction/reddening ratios are often associated with very massive stars as mentioned in Section 4.5. An extreme example is η Car, with high circumstellar extinction but only imperceptible reddening (Davidson & Humphreys 1997). Apparently the outflows from some massive stars produce unusually large grains, and, given SN 1954J's eruption, we should not be surprised if it belongs in that category.

The data are not adequate for a unique model, but here is a nearly satisfactory example. Suppose that the two stars have color temperatures $T_1 = 5000$ K and $T_2 = 20{,}000$ K; the former is indicated by the absorption lines, while the latter is more arbitrary, but a much hotter member is not supported[12] by the spectrum, Section 4.4. Further assume that the circumstellar extinction is 2.5 and 2.8 mag at $\lambda = 0.8\ \mu$m and 0.45 μm, respectively, and this applies equally to both stars and to the Hα emission. Then, by matching the corrected fluxes at 0.45 μm and 0.8 μm, we find the following results. The cool star has luminosity $L_1 \approx 3.6 \times 10^4\ L_\odot$, $M_{\rm bol} \approx -6.7$, and radius $R_1 \approx 250\ R_\odot$, while its hot companion has $L_2 \approx 2 \times 10^5\ L_\odot$, $M_{\rm bol} \approx -8.5$, and $R_2 \approx 37\ R_\odot$. The hot star contributes only about 30% of the continuum at $\lambda \approx 0.85\ \mu$m near the Ca II triplet (Figure 8). Its parameters appear satisfactory for an evolved massive star with mass loss and a continuing dense wind. Based on stellar models (Ekström et al. 2012), they correspond to initial masses for evolved stars of $\sim 20\ M_\odot$ and $\sim 15\ M_\odot$ for the hot and cool stars, respectively.

We do not know if this is a physical pair, but the G supergiant has been affected by some additional extinction, and therefore must be within the dust cloud, 4000–8000 au from the hot star. Based on stellar models with rotation (Ekström et al. 2012), a post-red supergiant of 20 $M_\odot$ near the end of its track, will be 10 million years old, while the somewhat lower mass G supergiant, $\sim 15\ M_\odot$, will be ~11–13 million years old, without or with rotation, respectively, in the stellar models. Given the uncertainties in the above model and the derived parameters, this is a reasonable agreement for a possible pair.

[12] Note that these are not effective temperatures. If the hot star has a Balmer jump, then its "effective" temperature may be somewhat less. However, we do not have sufficient data to quantify this detail.

The 20,000 K star is also suitable for producing the Hα feature. Given the hot star's radius, the observed $L(\mathrm{H}\alpha) \approx 1.4 \times 10^{37}$ erg s^{-1} can be emitted by a dense wind with density $n_e \sim 4 \times 10^{11}$ cm^{-3} just outside the photosphere. The corresponding Thomson-scattering depth is $\tau_{\rm sc} \approx 0.7$, which is nearly adequate for explaining the observed profile, given the various uncertainties. (Note that the Hα line played no role in calculating the star's radius.) Admittedly, we have not corrected for inhomogeneous "clumping" in the wind, but on the other hand it may be bipolar or equatorial, which can increase the relevant size of $\tau_{\rm sc}$. If the outflow velocity is 300 km s^{-1}, then the implied mass-loss rate for the stellar wind is of the order of $3 \times 10^{-5}\ M_\odot$ yr^{-1}.

Strictly speaking, the above model slightly violates the upper luminosity limit described in Section 4.5, based on the 24 μm flux from dust. But this is not a very serious objection, since many of the assumptions can easily be readjusted. For instance, the 24 μm argument fails if some light escapes through gaps in the dust. And the circumstellar extinction may be somewhat smaller than we have assumed, because the present-day hot star may be intrinsically somewhat fainter than it was before the eruption. (Having lost some mass and also some energy, it can now be slightly less luminous and appreciably hotter than it was then.) Given these uncertainties, the model described above confirms that a two-component interpretation of star 4 is feasible. Moreover, it is less arbitrary than the other concepts outlined in Section 4.4 above. Pending new evidence, we conclude that the survivor of SN 1954J is most likely an evolved blue supergiant, with a companion G-type supergiant. The blue supergiant most likely had an initial mass around 20 $M_\odot$. We suspect that it is a post-red supergiant, on a blue loop, and has lost about half of its initial mass so that its proximity to the Eddington Limit will reduce its stability (Humphreys & Davidson 1994; Davidson 2016).

This result is practically what one would expect for a giant eruption (Humphreys & Davidson 1994). It qualitatively resembles Van Dyk's (Van Dyk et al. (2005b) suggestion based on the same expectations from circumstellar dust. Kochanek et al. (2012) mentioned similar parameters for the likely progenitor but rejected it based on the dust properties.

A good signal-to-noise blue spectrum of this faint star is needed to further refine the physical characteristics of the likely hot star progenitor and to better understand its evolutionary state.

5. Summary and Discussion

Our two supernova impostors, SN 2002 kg and SN1954J, are survivors. Each was the eruption or high mass-loss event of an evolved massive star, but they have very different stories to tell.

SN2002kg or V37 is an LBV/S Dor-type variable. In 2002, it had a high mass-loss event and was initially classified as a Type IIn supernova with narrow hydrogen lines in emission. However, it was subluminous and was identified with V37 in NGC 2403 (Van Dyk 2005a; Weis & Bomans 2005), a known "irregular blue variable"(Tammann & Sandage 1968). Its pre-eruption colors show that V37 was a hot O9-B0 star. During its eruption, V37 formed a cool, dense wind with absorption lines typical of an early A-type supergiant in its spectra near maximum light, in addition to the strong, narrow hydrogen emission. Its light curve shows that its high mass-loss stage lasted about 13 years and it has nearly returned to its pre-eruption or quiescent magnitude. A current spectrum now

shows a much hotter star, as expected, with He I emission and P Cygni profiles due to its stellar wind. V37 also has a circumstellar nebula, which very likely formed during the recent eruption, although it did not form dust. We show that V37's pre-eruption luminosity and its luminosity near maximum was approximately $M_{\rm Bol} \approx 10.4$ mag or 10^6 $L_\odot$ and it had a probable initial mass of 60–80 $M_\odot$. Like other LBVs/S Dor variables, V37s outburst was an apparent transit on the HR Diagram, at nearly constant luminosity due to increased mass loss and the formation of a cooler, dense wind. With its luminosity and apparent temperature of ≈30,000 K from its intrinsic colors, V37 will lie on the LBV/S Dor instability strip (Wolf 1989; Humphreys & Davidson 1994) near classic LBVs such as R127 in the LMC.

Recently, Smith & Tombleson (2015) suggested that LBVs are "kicked mass gainers," i.e., former binary components that gained mass from pre-supernova companions and are now runaways. Their arguments were based on statistical isolation of LBVs from other massive stars, specifically O-type stars. Humphreys et al. (2016) found, however, that genuine luminous "classical LBVs" are not isolated, while the less luminous LBVs differ in this respect because they are substantially older. Altogether the spatial distributions agree with standard expectations. (Smith 2016 disputed these findings, but Davidson et al. (2016) listed specific invalid assumptions in each of his objections.) The most important outcome was strong arguments favoring the standard view of LBVs as evolved massive stars. How do V12 and V37 fit into this context? First, V37 is not isolated. It is in a spiral arm and associated with other reddened hot stars (Maund et al. 2006; Van Dyk et al. 2006), similar to the classical LBVs in our Local Group galaxies (Humphreys et al. 2016). V12 is not an LBV/S Dor variable. It was a giant eruption. Although it is a probable binary, there is no reason to require mass exchange as in the Smith & Tombleson (2015) model for LBVs. Furthermore, V12 is not isolated. It is in a spiral arm and its immediate environment (Figure 1) includes a hot supergiant, two red supergiants, and a G-type supergiant companion.

In its giant eruption, SN1954J/V12 increased by five magnitudes in apparent brightness and its absolute magnitude at maximum was at least −13 or $\approx 10^7$ $L_\odot$. Its maximum luminosity and its premaximum outbursts are similar to other SN impostors or giant eruptions.

Based on V12's pre-eruption light curve, we estimate an M_B of −7.2 for V12's progenitor, corrected for the interstellar extinction in its environment. With no color information at that time, we cannot directly estimate its temperature and luminosity. Assuming the approximate $B - V$ color of 1.0 observed during the rise to maximum, its luminosity was $\approx 10^5$ $L_\odot$ with an initial mass of 20 $M_\odot$. The likely survivor, the Hα bright star 4 in the *HST* images, however, is now 2.5 to 3 mag fainter than the pre-eruption progenitor with a luminosity of only $\approx 10^4$ $L_\odot$.

V12/star 4's red spectrum shows prominent Hα emission with an electron scattering stellar wind profile plus the Ca II triplet in absorption and neutral metallic lines of Fe I and Ti I. The absorption lines are consistent with a late G-type supergiant with a temperature of about 5000 K. V12's colors, however, are anomalous; too blue for a G-type star. Its SED is also peculiar and cannot be fit by a single 5000 K star. We therefore suggest that star 4 is actually two stars; a hotter star responsible for the Hα emission plus the G-type supergiant. Star 4's SED can be adequately fit by a two-component model with a hotter star in the temperature range of 15,000 to 25,000 K plus the 5000 K cooler star.

We also demonstrate that if the 24 μm flux in the V12 environment is the remnant radiation from V12's ejecta, the total mass shed in the eruption was ∼0.5 $M_\odot$. The 24 μm flux also sets constraints on the luminosity radiated by the dust, $L_{\rm IR} \sim 10^5$ $L_\odot$ comparable to most of the flux estimated for the progenitor star. Reradiation by dust can thus account for most of the apparent post-eruption decrease in the brightness of V12.

With additional circumstellar extinction, the hotter component, assuming a 20,000 K star, would have a luminosity of 2×10^5 $L_\odot$ comparable to that originally estimated for the progenitor star. If the G supergiant also suffers circmstellar extinction its corresponding luminosity would be $\approx 3.6 \times 10^4$ $L_\odot$.

Our analysis of these two impostors has revealed two very different stars. V37/SN2002kg is a classical LBV, an evolved massive star, 60–80 $M_\odot$, experiencing enhanced mass-loss episodes due to its proximity to its Eddington limit (Humphreys et al. 2016). Curiously, the much lower mass V12/SN1954J had the giant eruption, but its high mass-loss event was also fueled by its proximity to its Eddington limit. Based on our estimates for the temprature and luminosity of the hot star, V12 would lie just below the LBV instability strip on the HR Diagram. As has been suggested for the "less luminous" LBVs (Humphreys & Davidson 1994; Vink 2012), V12 was very likely a post-red supergiant that had evolved back to warmer temperatures. As a red supergiant, it would have lost a lot of mass bringing it closer to its Eddington limit and more subject to interior as well as surface instabilities. Stellar models (Ekström et al. 2012) with mass loss and rotation for 20 $M_\odot$ and 25 $M_\odot$ show that these stars, on a blue loop, would have shed half their initial masses when they reach the blue side of the HR Diagram. Interestingly, near the end of the model, the 20 $M_\odot$ track shows a short transit to the red, an ideal state for a star to experience a high mass-loss event as it tries to evolve to cooler temperatures. Finally, if the interpretation of the plateau on its declining light curve as a collision with previous ejecta is correct, then V12/SN1954J had experienced high mass events, even giant eruptions, in the past.

Research by R.H. and K.D. on massive stars is supported by the National Science Foundation AST-1109394. This paper uses data from the MODS1 and MODS2 spectrographs built with funding from NSF grant AST-9987045 and the NSF Telescope System Instrumentation Program (TSIP), with additional funds from the Ohio Board of Regents and the Ohio State University Office of Research.

Facilities: MMT/Hectospec, LBT/MODS1 + MODS2, *HST*/ACS, *HST*/WFC3.

ORCID iDs

Roberta M. Humphreys https://orcid.org/0000-0003-1720-9807
Schuyler D. Van Dyk https://orcid.org/0000-0001-9038-9950
Michael S. Gordon https://orcid.org/0000-0002-1913-2682

References

Auer, L. H., & Van Blerkom, D. J. 1972, ApJ, 178, 175
Binder, B., et al. 2015, AJ, 150, 94
Cardelli, J. A., Clayton, G. C., & Mathis, J. S. 1989, ApJ, 345, 245
Castelli, F., & Kurucz, R. L. 2004, in IAU Symp. 210, Modelling of Stellar Atmospheres, ed. N. Piskunov et al. (Cambridge: Cambridge Univ. Press), poster A20 (arXiv:astro-ph/0405087)
Cenarro, A. J., Cardiel, N., Gorgas, J., et al. 2001, MNRAS, 326, 959
Davidson, K. 1987, ApJ, 317, 760
Davidson, K. 2016, JPhCS, 728, 022008
Davidson, K., & Humphreys, R. M. 1997, ARA&A, 35, 1
Davidson, K., & Humphreys, R. M. 2012, Natur, 486, E1
Davidson, K., Humphreys, R. M., & Weis, K. 2016, arXiv:1608.02007
Davidson, K., et al. 1995, AJ, 109, 1784
Dessart, L, et al. 2009, MNRAS, 394, 21
Dolphin, A. E. 2000, PASP, 112, 1383
Eck, C. R., Cowan, J. J., & Branch, D. 2002, ApJ, 57, 306
Ekström, S., Georgy, C., Eggenberger, P., et al. 2012, A&A, 537, 146
Fabricant, D. G., Hertz, E. N., Szentgyorgyi, A. H., et al. 1998, Proc. SPIE, 3355, 285
Fabricant, D., et al. 2005, PASP, 117, 1411
Filippenko, A. V., & Chornock, R. 2003, IAUC, 8051, 2
Flower, P. J. 1996, ApJ, 469, 355
Freedman, W. L., & Madore, B. F. 1988, ApJ, 332, 63
Gordon, M. S., Humphreys, R. M., & Jones, T. J. 2016, ApJ, 826, 50
Humphreys, R. M., & Davidson, K. 1994, PASP, 106, 1025
Humphreys, R. M., Davidson, K., Gordon, M. S., et al. 2014a, ApJL, 782, L21
Humphreys, R. M., Davidson, K., Grammer, S., et al. 2013, ApJ, 773, 46
Humphreys., R. M., Davidson, K., Jones, T. J., et al. 2012, ApJ, 760, 93
Humphreys, R. M., Davidson, K., & Koppelman, M. 2008, AJ, 135, 1249
Humphreys., R. M., Davidson, K., & Smith, N. 1999, PASP, 111, 1124
Humphreys., R. M., Weis, K., Davidson, K., & Bomans, D. 2014b, ApJ, 790, 48
Humphreys, R. M., Weis, K., Davidson, K., & Gordon, M. S. 2016, ApJ, 825, 64
Keenan, P. C., & Hyneks, J. A. 1945, ApJ, 101, 265
Kochanek, C. S., Szczygiel, D. M., & Stanek, K. Z. 2011, ApJ, 737, 76
Kochanek, C. S., Szczygiel, D. M., & Stanek, K. Z. 2012, ApJ, 758, 142
Kowal, C. T., et al. 1972, PASP, 84, 844
Kraus, M., Cidale, L. S., Arias, M. L., Oksala, M. E., & Borges Fernandes, M. 2014, ApJL, 780, L10
Larsen, S. S., & Richtler, T. 1999, A&A, 345, 59
Makovoz, D., & Khan, I. 2005, in ASP Conf. Ser. 347, Astronomical Data Analysis Software and Systems XIV, ed. P. Shopbell, M. Britton, & R. Ebert (San Francisco, CA: ASP), 81
Makovoz, D., & Marleau, F. R. 2005, PASP, 117, 1113
Margutti, R., et al. 2014, ApJ, 780, 21
Martins, F., Schaerer, D., & Hillier, D. J. 2005, A&A, 436, 1049
Mauerhan, J. C., Smith, N., Filippenko, A. V., et al. 2013a, MNRAS, 430, 1801
Mauerhan, J. C., Smith, N., Silverman, J. M., et al. 2013b, MNRAS, 431, 2599
Maund, J. R., et al. 2006, MNRAS, 369, 390
Maund, J. R., et al. 2008, MNRAS, 387, 1344
Mehner, A., et al. 2013, A&A, 555, A116
Oksala, M. E., Kraus, M., Cidale, L. S., Muratore, M. F., & Fernandes, Borges. 2013, A&A, 558, A17
Owocki, S. P., & Shaviv, N. J. 2016, MNRAS, 462, 345
Pastorello, A., et al. 2010, MNRAS, 408, 181
Pastorello, A., et al. 2013, ApJ, 767, 1
Schlafly, E. F., & Finkbeiner, D. P. 2011, ApJ, 737, 103
Schwarz, M., & Li, W. 2003, IAUC, 8051
Sirianni, M., et al. 2005, PASP, 117, 1049
Smith, N. 2016, MNRAS, 461, 3353
Smith, N., Humphreys, R. M., & Gerhrz, R. D. 2001, PASP, 113, 692
Smith, N., & Tombleson, R. 2015, MNRAS, 447, 598
Smith, N., et al. 2010, AJ, 139, 1451
Suh, K.-W. 1999, MNRAS, 304, 389
Tammann, G. A., & Sandage, A. 1968, ApJ, 151, 825
Thé, P. S., & Graaland, F. 1995, RMxAC, 2, 75
Van Dyk, S. D. 2005a, in ASP Conf. Ser. 332, The Fate of the Most Massive Stars, ed. R. Humphreys & K. Stanek (San Francisco, CA: ASP), 49
Van Dyk, S. D., Filippenko, A. V., Chornock, R., Li, Weidong., & Challis, P. M. 2005b, PASP, 117, 553
Van Dyk, S. D., Li, Weidong., Filippenko, A. V., et al. 2006, arXiv:astro-ph/0603025v1
Van Dyk, S. D., & Matheson, T. 2012a, ApJ, 746, 179
Van Dyk, S. D., & Matheson, T. 2012b, in Eta Carinae and the Supernova Impostors, ed. K. Davidson & R. M. Humphreys (New York: Springer), 249
Vink, J. S. 2012, in Eta Carinae and the Supernova Impostors, ed. K. Davidson & R. M. Humphreys (New York: Springer), 221
Wagner, R. M., et al. 2004, PASP, 116, 326
Weis, K., & Bomans, D. J. 2005, A&A, 429, L13
Wolf, B. 1989, A&A, 217, 87
Wolf, B., Appenzeller, I., & Stahl, O. 1981, A&A, 103, 94